9. Supplementary Material

9.1 Deformation Gradient and Infinitesimal Strain

The deformation gradient was computed from two consecutive images using the nodal displacements obtained from the texture correlation algorithm. The finite element of shape function interpolation was used:

$$dF_{iJ} = \sum_{a=1}^{4} x_{a,i} \frac{\partial N_a}{\partial X_J}, \tag{SI 1}$$

where $\partial N_a/\partial X_J$ is the derivative of the a'th shape function with respect to the reference configuration and $x_{a,i}$ are the deformed nodal coordinates for the a'th node. In order to obtain the total deformation gradient for a given step, the differential deformation gradient from all previous loading steps were multiplied:

$$\mathbf{F}_N = \prod_{i=1}^{N} \mathbf{dF}_i . \tag{SI 2}$$

The infinitesimal strain tensor was then computed from the deformation gradient:

$$\boldsymbol{\varepsilon} = \frac{1}{2}\left[\left(\mathbf{F}_N - \mathbf{I}\right) + \left(\mathbf{F}_N - \mathbf{I}\right)^T \right]. \tag{SI 3}$$

9.2 Gel and Fiber Constitutive Model and Curve Fitting

The constitutive model consisted of an elliptical fiber distribution embedded within a matrix material (Ateshian et al. 2009). This model was used to describe the material behavior of the collagen gels and extruded fibers. The Cauchy stress $\boldsymbol{\sigma}$ is the sum of fiber and matrix stresses:

$$\boldsymbol{\sigma} = \boldsymbol{\sigma}^f + \boldsymbol{\sigma}^m . \tag{SI 4}$$

Both terms are defined by strain energy functions:

$$\boldsymbol{\sigma}^f = \int_0^{2\pi}\int_0^{\pi} H\left(\lambda_n - 1\right) 2J^{-1}\mathbf{F}\frac{\partial W^f}{\partial \mathbf{C}}\mathbf{F}^T \sin\phi \, d\phi \, d\theta , \tag{SI 5}$$

$$\boldsymbol{\sigma}^m = 2J^{-1}\mathbf{F}\frac{\partial W^m}{\partial \mathbf{C}}\mathbf{F}^T , \tag{SI 6}$$

where $\boldsymbol{\sigma}^f$ requires an integration over a unit sphere. Because of the Heaviside function, $H\left(\lambda_n - 1\right)$, the fibers contribute in tension only. The strain energy functions are defined as:

$$W^f\left(\mathbf{n}^r,\lambda_n^2\right)=\xi\left(\mathbf{n}^r\right)\left(\lambda_n^2-1\right)^{\alpha\left(\mathbf{n}^r\right)}, \tag{SI 7}$$

$$W^m\left(I_1\right)=\frac{E}{2\left(1+\nu\right)}\left(I_1-3\right). \tag{SI 8}$$

The fiber stretch, λ, is defined as:

$$\lambda_n=\sqrt{\mathbf{n}^r\cdot\mathbf{C}\cdot\mathbf{n}^r}, \tag{SI 9}$$

where $\mathbf{C}$ is the right Cauchy deformation tensor and $\mathbf{n}^r$ is the major axis of the elliptical fiber distribution, which determines the fiber modulus ξ and the power law coefficient α:

$$\xi\left(\mathbf{n}^r\right)=\left(\frac{\cos\left(\Theta\right)^2\sin\left(\Phi\right)^2}{\xi_1^2}+\frac{\sin\left(\Theta\right)^2\sin\left(\Phi\right)^2}{\xi_2^2}+\frac{\cos\left(\Phi\right)^2}{\xi_3^2}\right)^{-1/2}, \tag{SI 10}$$

$$\alpha\left(\mathbf{n}^r\right)=\left(\frac{\cos\left(\Theta\right)^2\sin\left(\Phi\right)^2}{\alpha_1^2}+\frac{\sin\left(\Theta\right)^2\sin\left(\Phi\right)^2}{\alpha_2^2}+\frac{\cos\left(\Phi\right)^2}{\alpha_3^2}\right)^{-1/2}, \tag{SI 11}$$

and

$$\mathbf{n}^r=\cos\Theta\sin\Phi\,\mathbf{a}_1+\sin\Theta\sin\Phi\,\mathbf{a}_2+\cos\Theta\,\mathbf{a}_3. \tag{SI 12}$$

A coordinate transformation must be performed between the local coordinate basis ($\mathbf{a}_i$) and the global basis ($\mathbf{e}_i$) to relate $\left(\Phi,\Theta\right)$ and $\left(\phi,\theta\right)$. The coefficients α_1, α_2, α_3 and ξ_1, ξ_2, ξ_3 represent the major and minor axes of an ellipsoidal distribution.

The model has a total of eight coefficients: E, ν, α_1, α_2, α_3, ξ_1, ξ_2 and ξ_3. The matrix modulus E and Poisson's ratio ν are related, since the term $\frac{E}{2\left(1+\nu\right)}$ in Equation SI 8 is the shear modulus. If ν is set to zero, E is only independent matrix coefficient. Further simplifications can be made if information is known regarding the fiber distributions for the material. SEM imaging of collagen gels reveals an isotropic distribution of fibrils (Fig. S4). The precise organization of the gel can be obtained by finding the angular fiber distribution via the use of a polar Fast Fourier Transform (FFT) (Chang 2011). The anisotropy of SEM images of collagen gels ranged between 0.05-0.15, indicating a nearly random distribution (Fig. S4). With these observations, the following reductions are reasonable: $\alpha_1=\alpha_2=\alpha_3=\alpha_{gel}$, and $\xi_1=\xi_2=\xi_3=\xi_{\mathrm{gel}}$. This leaves three unique

coefficients: E_{gel}, α_{gel}, and ξ_{gel}. For the extruded collagen fiber, FFT analysis of SEM images revealed an anisotropic fiber distribution (Fig. S4), with anisotropy ranging from 0.6-0.8. The ratio of the major and minor axis of these fiber distributions is ~4. Thus, the ξ coefficients were given a transversely isotropic distribution, $\xi_1 = \xi_2 = \xi_{xy}$, $\xi_z = 4\xi_{xy}$. The power law coefficients were assumed to be isotropic, $\alpha_1 = \alpha_2 = \alpha_3 = \alpha_{fiber}$. For the extruded fibers, a total of 3 unique coefficients must be found. A nonlinear, constrained global optimization routine (a pattern search algorithm) was implemented in Matlab that found the coefficients that minimized the sum of squares difference between the experimental curves and the fit curves. Two datasets were used simultaneously for the curve fits: uniaxial stress-strain data and 2D axial strain-transverse strain data. The fit results were relatively insensitive to starting values. Curve fits were performed for each individual fiber and gel, and for the average test data (Table S1).

9.3 Sensitivity of Micromechanical FE Model to Aspect Ratio

To explore boundary effects, micromechanical models were created with aspect ratios (AR) of 4:1, 8:1, 16:1, 24:1, 40:1 and 80:1. These models were analyzed with the same material properties and boundary conditions as described previously. To simulate a surrogate with an infinite aspect ratio, a simulation of unconstrained uniaxial tension was performed by removing the displacement constraints in the lateral direction. To assess homogeneity in the strain field, the microscale transverse strains at the model center in the x-z plane were extracted for both the constrained model (AR=8:1) and the unconstrained model, with the coefficient of variation being computed for each model.

9.4 Continuum FE Model

If the continuum assumption is valid for the surrogates, then a FE model that represents the fibers and matrix together using a homogenized set of material coefficients should produce similar results to those obtained for the micromechanical FE models for all aspect ratios. To test whether the continuum assumption would be reasonable, the macroscopic stress and macroscopic 2D strain for the composite surrogate material were curve fit with the EFD model, using the same procedure as described for the fibers and gel. The resulting

homogenized material coefficients were used for both the fiber and matrix materials in the FE models with varying aspect ratio.

9.5 Sensitivity Studies

To assess model sensitivity to inter-fiber spacing, models with an aspect ratio of 10:1 (typical aspect ratio for tendon or ligament) were created with a constant fiber diameter (185 μm) and a varied inter-fiber spacing (10, 20, 60, 160, 300 μm). To assess model sensitivity to the ratio of fiber stiffness to gel stiffness, the stiffness of the gel for the 10 μm spacing model was scaled by 1-500 while the fiber stiffness was held constant. This provided a ratio of fiber stiffness to gel stiffness (E_{fiber}/E_{matrix}) ranging from 8-2500. The difference between the microscale transverse fiber strain and the microscale transverse matrix strain:

$$\Delta\varepsilon_{micro} = \varepsilon_{trans}^{Matrix} - \varepsilon_{trans}^{Fiber} \quad \text{(SI 13)}$$

was used to assess inhomogeneity in the microscale strain field.

9.6 Normalized Root Mean Square Error

The normalized root mean square was used to compare the experimentally measured stress and strain values to those obtained from the micromechanical FE models. It was defined as:

$$NRMSE = \left(\frac{1}{\max\left(x^{Exp}\right) - \min\left(x^{Exp}\right)} \right) \sqrt{\frac{\sum_{i=1}^{N}\left(x_i^{Exp} - x_i^{FE}\right)}{N}}, \quad \text{(SI 14)}$$

where x^{Exp} is the experimental value and x^{FE} is the corresponding value obtained from the FE simulation.

9.7 Coefficient of Variation

The coefficient of variation was used as a metric for inhomogeneity in the microscale transverse strain, where a larger percentage corresponds to increased inhomogeneity and a lower percent corresponds to a decrease in inhomogeneity. It was defined as:

$$C_v = \frac{std\left(\varepsilon_{trans}\right)}{mean\left(\varepsilon_{trans}\right)}, \quad \text{(S15)}$$

where the standard deviation and mean was computed for all microscale transverse strain values within the cross section of the micromechanical FE model.

9.8 Supplementary Material Figure Legends

Figure S1. Gel and fiber curve fits. The continuous fiber model accurately described the stress-strain (upper left) and 2D strain (upper right) of the collagen gels (R^2=0.98). The continuous fiber model also described the stress-strain (lower left) and 2D strain (lower right) of the extruded fibers (R^2=0.99). In all plots the interpolated data points (with error bars) are black and the best fit curve is black.

Figure S2. Sensitivity studies. (Left) As the interfiber distance was decreased, the difference between the fiber and matrix strain increased. The surrogate spacing is circled in black, while the physialogically relvent values are boxed in red. (Right) For a constant interfiber spacing of 10 μm, an increase in the ratio of the fiber stiffness to the matrix stiffness resulted in a larger microscale strain difference between the fiber and matrix. The value corresponding to the surrogate matrix is circled in black, while the physiologically relevent values are boxed in red.

Figure S3. Mechanical testing and FE mesh. (A) A custom test apparatus was mounted onto an inverted confocal microscope. The linear stage and load cell were interfaced to a PC via Labview. The sample was tested in a water chamber and images were acquired using confocal fluorescence imaging. (B) Collagen gels were molded into dog bone shaped specimens for uniaxial tensile testing where the 2D strain (the longitudinal strain and transverse strain) as well as the stress was measured. (C) A micromechanical FE model of the surrogate was constructed, where green elements represent the fibers and red elements represent the gel matrix.

Figure S4. EFD constitutive model. Three unique coefficients were needed to describe the gel and fiber behavior (Far left). SEM imaging revealed a random orientation of fibrils within gels (Top, center left) and an aligned orientation within fibers (Bottom, center left). FFT analysis was used to generate polar plots of the fiber distribution as well as the magnitude of the minor and principle axis. For the collagen gels, the ratio of the major to minor principle axis was nearly 1 (Top, center right), which is consistent with the assumption of a spherical fiber distribution (Top, far right). For the extruded fibers, the ratio of the major axis to

the minor axis was approximately 4:1 (Bottom, center right), which is consistent with the assumption of an elliptical fiber distribution (Top, far right). The local fiber direction, $\mathbf{n}^r$, is shown on the fiber distribution plots.

9.9 Supplementary Material Table

Table S1: EFD best fit coefficients. The best fit coefficients for the gel and fiber are given to three significant figures. Note that the parameter ξ_z was not fit independently; rather, it was computed from ξ_{xy}.

Fit	**E (MPa)**	**α**	**ξ_{xy}**	**ξ_z**	**R^2**
Gel	0.00160±.00060	3.02±.093	0.136±0.096	0.136±0.096	0.98
Fiber	2.67±1.79	2.24±.042	18.8±3.05	75.2±12.2	0.99

9.10 Supplementary Material Figures

Fig. S1

(page width)

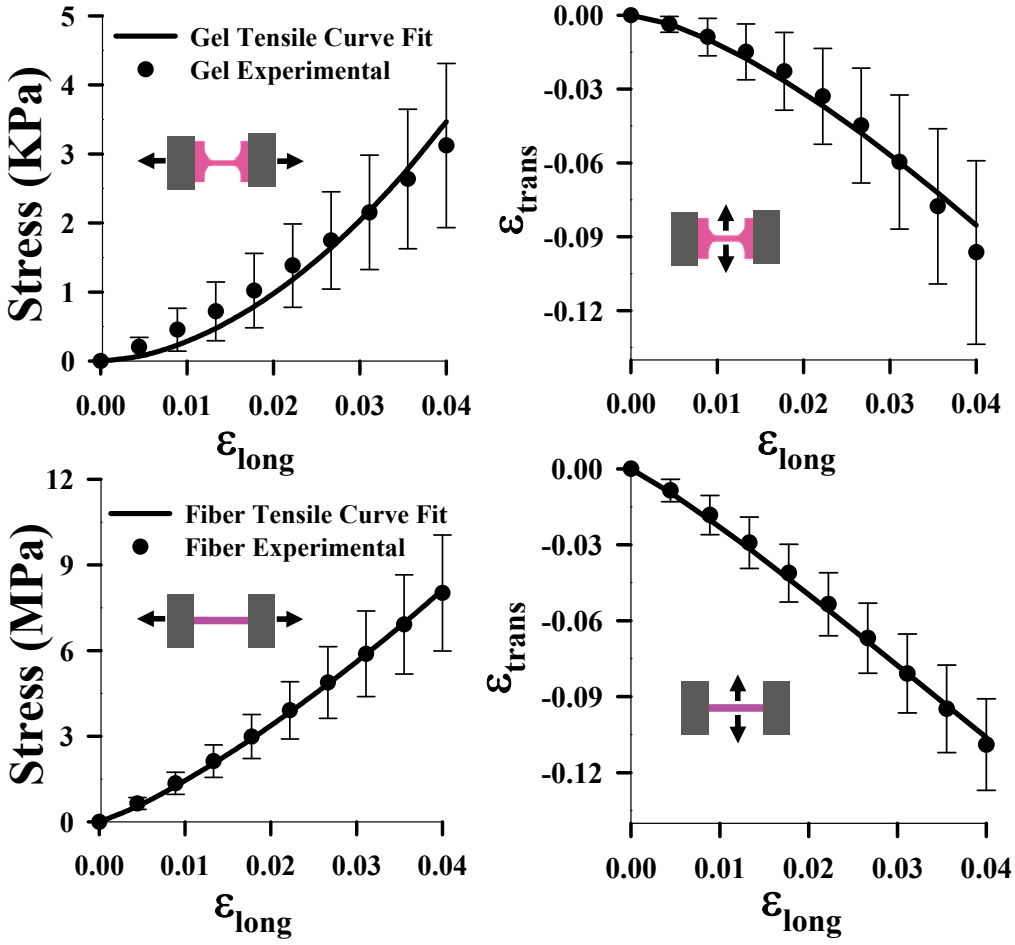

5

Fig. S2

(page width)

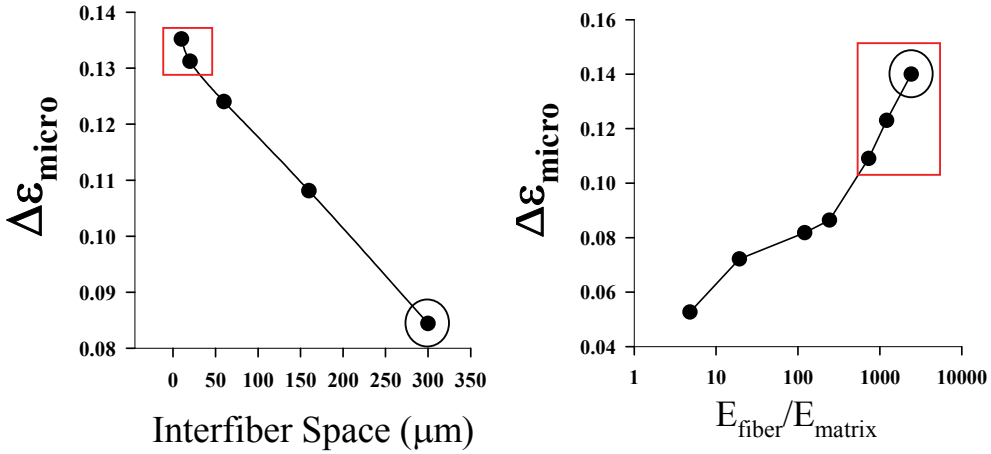

Fig. S3

(page width)

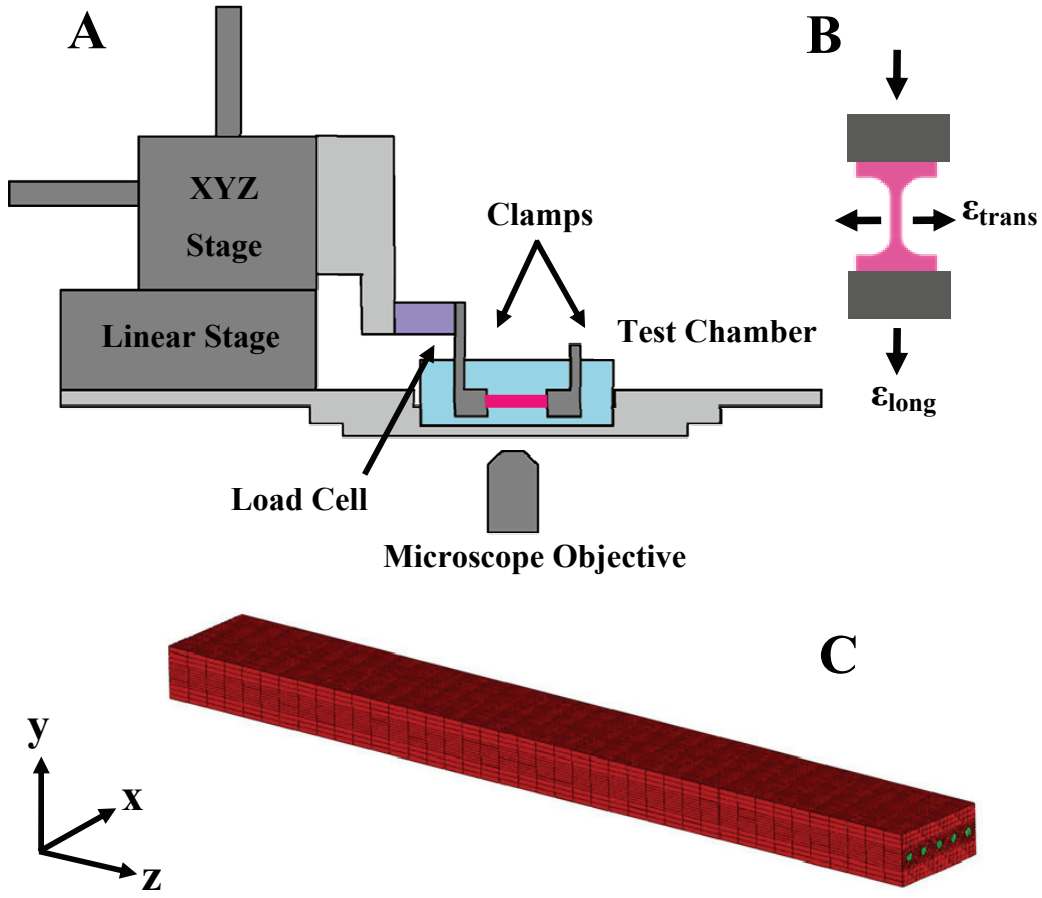

Fig. S4

(page width)